EXTRACTING GEOMETRICAL FEATURES & PEAK FRACTIONAL ANISOTROPY FROM THE ODF FOR WHITE MATTER CHARACTERIZATION

Aurobrata Ghosh, Rachid Deriche

EXTRACTING GEOMETRICAL FEATURES & PEAK FRACTIONAL ANISOTROPY FROM THE ODF FOR WHITE MATTER CHARACTERIZATION

Aurobrata Ghosh and Rachid Deriche

Project Team Athena, INRIA Sophia Antipolis-Méditerranée, France

ABSTRACT

Spherical Functions (SF) play a pivotal role in Diffusion MRI (dMRI) in representing sub-voxel-resolution micro-architectural information of the underlying tissue. This information is encoded in the geometric shape of the SF. In this paper we use a polynomial approach to extract geometric characteristics from SFs in dMRI such as the maxima, minima and saddle-points. We then use differential geometric tools to quantify further details such as principal curvatures at the extrema. Finally we propose new scalar measures like the Peak Fractional Anisotropy (PFA) and Total-PFA, to represent this rich source of information for characterizing white-matter (WM) fibers. As an example we illustrate our method on the Orientation Distribution Function (ODF) estimated from real data.

Index Terms— ODF, Tractography, Maxima, Principal Curvatures, Peak Fractional Anisotropy

1. INTRODUCTION

Diffusion Tensor Imaging (DTI) [1, 2] uses ellipsoids as SFs to represent the diffusion of water molecules in heterogeneous cerebral tissue to quantify its micro-architecture *in-vivo* and *non-invasively*. The spectral decomposition of the diffusion tensor into its eigenvalues and eigenvectors represents the ellipsoid's geometry. These and derived scalars indicate tissue micro-architecture such as the dominant fiber direction, parallel and perpendicular diffusion, mean diffusion and Fractional Anisotropy (FA) [2]. However, DTI is known to be inherently limited in regions where multiple fibers cross, kiss or diverge.

An example of functions capable of representing richer geometries on the sphere is the Orientation Distribution Function (ODF) by Tuch [3], which is the radial integral of the diffusion ensemble average propagator (EAP). It overcomes the limitation of DTI and can discern complex fiber configurations. We call this the ODF-T (Tuch). It is not a true angular marginal distribution obtained from the EAP, and needs to be numerically normalized. An analytical approach for computing the ODF-T, in the Spherical Harmonic (SH) basis, was proposed in [4]. An analytical approach for computing the true angular marginal distribution obtained from the EAP, with solid angle consideration in the radial integral, was

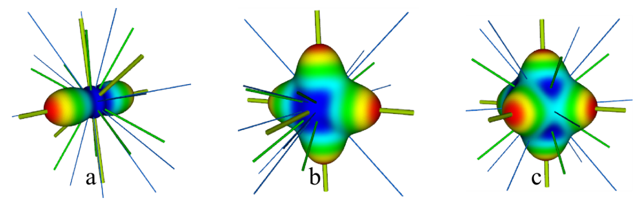

Fig. 1. Extrema extraction & categorization from synthetic data. a) 1-fiber b) 2-fibers c) 3-fibers. Glyph-colour: red indicates high anisotropy (local peak), blue indicates low anisotropy (local trough). Line-colour: thick-green: Maxima, thin-green: Minima, fine-blue: Saddle points

proposed, also in the SH basis, in [5, 6]. We call this the ODF-SA (Solid Angle). However, unlike in DTI, there exists no simple method for extracting all the geometric characteristics from these SFs with multiple extrema. Simple discrete mesh searches [4] and optimization approaches [7, 8] have been proposed for extracting only the maxima, but these are heuristic. Mathematically systematic approaches quantifying all the geometric characteristics are few [9, 10, 11].

In this paper we propose to extend and apply our polynomial approach for extracting the extrema of a SF [10]. As proposed in [9], using differential geometric tools, we also compute principal curvatures to further quantify the geometry of the extrema. Finally using the same tools, we propose new scalar measures like the Peak Fractional Anisotropy (PFA) and Total-PFA, to represent this rich source of geometric information for characterizing white-matter (WM) fibers. To illustrate, we experiment on ODF-Ts & ODF-SAs, estimated from real data and show important gains over existing scalar measures for complex SFs such as the GFA [3]. Although both are ODF models, ODF-SAs are known to have sharper peaks, and to detect more crossings than ODF-Ts, but are also more sensitive to signal noise.

2. THEORY

Extracting the geometric characteristics of a generic SF can be broken down into 3 steps. In the first, we represent the SF as a Homogeneous Polynomial (HP) constrained to a sphere. In the second, we optimize a constrained polynomial by solving a system of polynomials whose roots are the extrema of the SF and which can be bracketed analytically and computed numerically with high precision. In the third, we classify the extrema as maxima, minima and saddle-points and compute their principal curvatures to completely quantify all the extrema of the SF.

The SH basis is an ideal formulation for describing SFs and is widely used in dMRI to represent the diffusion SF. There exists a linear bijection transformation between the SH basis of rank-d and the HP basis of degree-d [12]. The SH transform of the HP can be represented by an invertible matrix $\mathbf{M}$ whose form is found in [12]. Therefore, the SF, which is estimated in the SH basis can be re-written as a HP constrained to the sphere, ($||\mathbf{x}||_2 = 1$):

$$\begin{aligned} \mathbf{M}^{-1}\mathbf{C} &= \mathbf{A} \\ \mathrm{P}(\mathbf{x} = [x_1, x_2, x_3]^T) &= \sum_{i+j+k=d} A_{i_1 i_2 i_3} x_1^i x_2^j x_3^k, \end{aligned} \quad (1)$$

where the SF's coefficients are $\mathbf{C}$ in the SH basis and $\mathbf{A}$ in the HP basis.

The extrema of the SF can be computed by maximizing $\mathrm{P}(\mathbf{x})$ on the sphere, formulated using Lagrange multipliers as an unconstrained functional $F(\mathbf{x}, \Lambda) = \mathrm{P}(\mathbf{x}) - \Lambda\,(\|\mathbf{x}\|_2^2 - 1)$. The extrema are roots of the functional's gradient, which is a system of polynomials:

$$\frac{\partial F}{\partial x_1} = \frac{\partial F}{\partial x_2} = \frac{\partial F}{\partial x_3} = \|\mathbf{x}\|_2^2 - 1 = 0. \quad (2)$$

Instead of solving the optimization problem, which can only be local at best, we identify all the real roots of the system (2) together using [13]. The polynomials are first converted to the Bernstein basis using exact arithmetic. Then a strategy of domain subdivision and reduction is used based on the properties of Bernstein polynomials, which allow an analytical bracketing of the roots in the domain by counting the number of sign changes of the coefficients. Thus by subdividing an initial domain known to contain all the real roots of the system, it is possible to analytically bracket all the roots. Then an efficient numerical approach is used to compute the roots precisely. All the roots are found together.

The extrema can be classified into maxima, minima and saddle-points using two distinct approaches. We use the Bordered Hessian (BH) approach [14] which resembles the typical Hessian definiteness condition in the case of an unconstrained optimization. However since the problem concerns a constrained optimization, the Hessian (H) of the functional $F(\mathbf{x}, \Lambda)$ is bordered by the first order derivatives of the constrain and padded by a corner-block of zeros to produce the BH ($\overline{H}$):

$$\overline{H}_{m+n}[F(\mathbf{x}, \Lambda)] = \left[\begin{array}{cc} 0_{m\times m} & B_{m\times n} \\ B^T_{m\times n} & H[F(\mathbf{x}, \Lambda)]_{n\times n} \end{array} \right] \quad (3)$$

where $B_{m\times n} = \frac{\partial(\|\mathbf{x}\|_2^2 - 1)}{\partial \mathbf{x}}$, $n = 3$: dimension of the problem, $m = 1$: number of constrains. The BH is rank deficient and cannot satisfy the definiteness condition of the Hessian except under certain conditions [14]. However, alternating sign conditions on the determinants of the principal sub matrices provide the BH conditions for classifying maxima, minima and saddle points:

$$\begin{aligned} (-1)^m|\overline{H}_r[F(\mathbf{x}, \Lambda)]| &> 0 \text{ strict minimum}, \quad (4) \\ (-1)^r|\overline{H}_r[F(\mathbf{x}, \Lambda)]| &> 0 \text{ strict maximum}, \quad (5) \\ & r = m+1, ..., n. \end{aligned}$$

Alternatively the formulae for computing the coefficients of the first and second fundamental forms in [9] can be used to compute the principal curvatures and classify the extrema from their signs. We also compute the principal curvatures κ_1, κ_2 to further quantify the geometry of the extrema after classification.

3. EXPERIMENTS AND RESULTS

We can extract all the geometric characteristics of a SF, namely the extrema and their principal curvatures, and also classify them. From these we propose new scalar measures to characterize WM fibers. To characterize each of the peaks (maxima) of the SF we propose the Peak Fractional Anisotropy (PFA) which is analogous to FA in DTI. To characterize the entire SF we consider the sum of all the PFAs corresponding to all the peaks of the SF and name it the Total-PFA.

PFA, is a new measure, that integrates the principal curvatures and function value for each maximum into a single scalar value. Essentially we fit an ellipsoid at every maximum, such that its principal axis corresponds to the maximum-direction, principal radius equals the maximum's function value, and principal curvatures along the principal axis equal the curvatures of the SF at the maximum. This allows us to define the eigenpair of the symmetric positive definite matrix of the ellipsoid. The PFA is the FA of this ellipsoid. We name this the Ellipsoid PFA (PFAe) corresponding to the maximum-peak.

We propose two other PFAs, each corresponding to the underlying SF model – ODF-T and ODF-SA, and call these the PFA-T and PFA-SA. If we consider anisotropic free diffusion, which corresponds to diffusion due to a single fiber, where the EAP is an oriented Gaussian parameterized by the diffusion tensor $\mathbf{D}$ (like DTI), then it is possible to compute the ODF-T and the ODF-SA of this EAP analytically. Let these analytical ODFs be known as the FD-ODF-T and the FD-ODF-SA, where FD indicates free diffusion. These are also parameterized by the diffusion tensor $\mathbf{D}$, and have only one maximum (single fiber). When $\mathbf{D}$ is taken in its canonical representation, it only has three parameters, namely its eigenvalues $\{\Lambda_i\}$, along the coordinate axes. In such a case, it is simple to compute the function value and the principal curvatures of the analytical FD-ODF-T and FD-ODF-SA at their maximum. By matching these to the maximum function value, and the principal curvatures of the peak of the SF under consideration, it is possible to fit an FD-ODF-T or an FD-ODF-SA to the peak, and to estimate $\mathbf{D}$.

Naturally, the model of the analytical ODF has to match the model of the SF, i.e. if the SF were an ODF-T, we match a FD-ODF-T to each of its peaks, and similarly if the SF were an ODF-SA, we match a FD-ODF-SA to each of its peaks. The FA of the diffusion tensor $\mathbf{D}$ estimated in this fashion for a peak, defines the PFA of that peak based on the model. In other words if the SF were an ODF-T, then the corresponding PFA for every peak is the PFA-T. And if the SF were an ODF-SA, then the PFA for every peak is the PFA-SA.

We now derive these analytical quantities. The maximum function value and principal curvatures of a canonically represented ellipsoid, parameterized by the diffusion tensor $\mathbf{D} = diag(\Lambda_x, \Lambda_y, \Lambda_z)$ elongated along the x-axis can be computed to be:

$$\begin{aligned} \kappa_1 &= \frac{\Lambda_x(3\Lambda_z - 2\Lambda_x)}{\Lambda_z};\ \kappa_2 = \frac{\Lambda_x(3\Lambda_y - 2\Lambda_x)}{\Lambda_y}; \\ \mathcal{F} &= \frac{1}{\Lambda_x}. \end{aligned} \tag{6}$$

These formulae can be used to fit an ellipsoid to the maximum value $\tilde{\mathcal{F}}$ and principal curvatures $\tilde{\kappa_1}, \tilde{\kappa_2}$ of a peak of the SF. Solving for $\Lambda_x, \Lambda_y, \Lambda_z$:

$$\begin{aligned} \Lambda_x &= \frac{1}{\mathcal{F}}; \\ \Lambda_y &= \frac{2}{\mathcal{F}(3 - \kappa_1\mathcal{F})}; \quad \Lambda_z = \frac{2}{\mathcal{F}(3 - \kappa_2\mathcal{F})}, \end{aligned} \tag{7}$$

it is then possible to compute the PFAe of the peak.

The analytical formula for a FD-ODF-T parameterized by $\mathbf{D}$, represented canonically, is found to be [15]:

$$\Psi_T(x, y, z) = \frac{1}{Z}\sqrt{\frac{1}{\frac{x^2}{\Lambda_x} + \frac{y^2}{\Lambda_y} + \frac{z^2}{\Lambda_z}}}, \tag{8}$$

where all the constants have been absorbed into Z, where Z is the normalizing constant since ODF-T isn't a true marginal distribution, and $\{\Lambda_i\}$ are the eigenvalues of $\mathbf{D}$. The maximum function value and principal curvatures can also be computed analytically when Ψ_T or $\mathbf{D}$ is elongated along the x-axis. The quantities are found to be:

$$\kappa_1 = \frac{Z\sqrt{\Lambda_x}}{\Lambda_y};\ \kappa_2 = \frac{Z\sqrt{\Lambda_x}}{\Lambda_z};\ F = \frac{\sqrt{\Lambda_x}}{Z}. \tag{9}$$

Eq-9 implies that the $\{\Lambda_i\}$ can be computed uniquely only up to the constant Z. But since scaling the eigenvalues doesn't change the FA, we can fix $Z = 1$ and solve for $\Lambda_x, \Lambda_y, \Lambda_z$:

$$\begin{aligned} \Lambda_x &= \mathcal{F}^2; \\ \Lambda_y &= \frac{\mathcal{F}}{\kappa_1}; \quad \Lambda_z = \frac{\mathcal{F}}{\kappa_2}. \end{aligned} \tag{10}$$

These can be used for fitting a FD-ODF-T to each peak of any ODF-T, when its function value and principal curvatures $\tilde{\mathcal{F}}, \tilde{\kappa_1}, \tilde{\kappa_2}$, are known, making it possible to compute the peak's PFA-T from the $\{\Lambda_i\}$.

Similarly the analytical formula for a FD-ODF-SA parameterized by $\mathbf{D}$, represented canonically, can be computed to be:

$$\Psi_{SA}(x, y, z) = \frac{1}{4\pi\sqrt{\Lambda_x\Lambda_y\Lambda_z}}\left(\frac{1}{\frac{x^2}{\Lambda_x} + \frac{y^2}{\Lambda_y} + \frac{z^2}{\Lambda_z}}\right)^{\frac{3}{2}}. \tag{11}$$

This is a true marginal distribution and, therefore, doesn't have a normalizing constant. The formulae for the maximum function value and principal curvatures can again be computed analytically when Ψ_{SA} is elongated along the x-axis. We find:

$$\begin{aligned} \kappa_1 &= \frac{4\pi\Lambda_y(3\Lambda_x - 2\Lambda_z)}{\Lambda_x\sqrt{\Lambda_y\Lambda_z}};\ \kappa_2 = \frac{4\pi\Lambda_z(3\Lambda_x - 2\Lambda_y)}{\Lambda_x\sqrt{\Lambda_y\Lambda_z}} \\ \mathcal{F} &= \frac{\Lambda_x^{3/2}}{4\pi\sqrt{\Lambda_x\Lambda_y\Lambda_z}}, \end{aligned} \tag{12}$$

Interestingly, Eq-12 indicates that the function value and principal curvatures, at the maximum of a FD-ODF-SA, remain unchanged if the $\{\Lambda_i\}$ are multiplied by a constant. Therefore, again, Eq-12 can be solved for $\Lambda_x, \Lambda_y, \Lambda_z$ only up to a scaling factor. However, since that doesn't change the computed FA, we consider the solution set:

$$\begin{aligned} \Lambda_x &= 1; \\ \Lambda_y &= \frac{3}{\kappa_2\mathcal{F} + 2}; \quad \Lambda_z = \frac{3}{\kappa_1\mathcal{F} + 2}. \end{aligned} \tag{13}$$

These can be used for fitting a FD-ODF-SA to each peak of any ODF-SA, and to compute the PFA-SA of the peak from the $\{\Lambda_i\}$.

The various PFAs allow us to naturally characterize each peak of a SF. We simply extend this characterization to the entire SF by considering a weighted sum the PFAs for all its peaks. We designate this the Total-PFA (Total-PFAe, Total-PFA-T and Total-PFA-SA):

$$\mathrm{TotalPFA} = \sum_{i=1}^{N} \mathcal{F}_i \cdot \mathrm{PFA}_i.$$

Since the Total-PFA is a summation of all the local anisotropy measure from each peak, it is therefore an integrated measure of the overall peakedness of a SF. It indicates how star-like the shape of the SF is.

3.1. Results

Fig-1 shows results of extrema extraction and classification on ODF-Ts estimated from fiber-crossing signals generated synthetically using a multi-tensor model for 1, 2 and 3 fibers crossing perpendicularly. In case of the 1 and 2 fiber models we note that unimportant local maxima are also correctly detected and would need to be thresholded, since these do not represent fiber directions, and were inherently generated by the estimation process. In real data, a similar situation can arise when due to noise the estimation can generate spurious peaks that do not represent true fiber directions. These are often thresholded heuristically.

In Fig-2 we present a coronal slice with the ODF-Ts and ODF-SAs along with the extracted maxima. We note the marked increase in voxels with fiber crossings detected by ODF-SA, which are known to have sharper peaks [5]. Further, even though the peaks in the ODF-T are subtle (indicated by the glyph colour), the maxima extraction method is still able to detect these. The ODFs (ODF-T & ODF-SA) were estimated from a real dataset [16].

Fig-3 compares the DTI RGB map with FA as brightness, to the dominant maximum of ODF-T (ODF-SA) with the corresponding PFA-T (PFA-SA) as brightness. The striking similarity between the three RGB maps indicates the validity of the maxima extraction process.

Finally the results of Total-PFA are presented in Fig-4. Three types of scalar measures are presented in this figure to highlight the sensitivity of Total-PFA. The first column is the GFA, the second column is the Total-PFA, and the third column is an image where the contrast is the number of maxima in the ODF-Ts and ODF-SAs. The first row contains the results from ODF-Ts, and the second row contains results from ODF-SAs. The arrows indicate regions that highlight the sensitivity of Total-PFA.

The green arrows indicate regions where the ODF models have only a single maximum (dark in the number-of-maxima image: 3rd column), and where these single maxima display high anisotropy (bright in the Total-PFA: 2nd column). These are typically in the CC and the CST, and are also bright in the GFA (1st column). The orange arrows indicate regions where the ODF models have multiple peaks (bright in the 3rd column), and where these multiple maxima have low anisotropy (dark in the Total-PFA: 2nd column). These regions are dark in the GFA too (1st column). The red arrows indicate regions where the ODF models again have multiple peaks (again bright in the 3rd column), but this time these multiple maxima have high anisotropy (bright in the Total-PFA: 2nd column). However, these regions appear dark in the GFA (1st column), just like the regions indicated by the orange arrows in the GFA. These are typically regions with crossing fibers – like where the CC, the CST and the SLF intersect. Therefore, these are regions that tend to have high local anisotropy.

This shows that Total-PFA, with its emphasis on subvoxel local anisotropy can highlight regions of the underlying tissue that have complex microstructures. Since Total-PFA sums the PFAs of all the peaks of an SF, where the PFAs measure the individual anisotropy of the peaks, Total-PFA is able to discern between regions with multiple peaks and low peak anisotropies, which should intuitively correspond to globally isotropic SFs, and regions with multiple peaks and high peak anisotropies, which are regions with high local anisotropies along multiple directions. Such regions occur when fibers cross, and where the SFs have pronounced star-like shapes

4. CONCLUSIONS

In this paper we extracted the geometric characteristics of a SF, classified them as maxima, minima and saddle-points, and computed their principal curvatures. Using this rich source of information we proposed the PFA and Total-PFA to characterize cerebral tissue since they incorporate the geometric characteristics of the SF. In the future we would like to explore fiber tractography on ODFs where we use PFA and Total-PFA as tracking criterion to compare the results with FA and GFA in fiber-tracking.

Acknowledgements This work was partially supported by the ANR project NucleiPark and the France-Parkinson Association.

5. REFERENCES

[1] P.J. Basser, J. Mattiello, and D. LeBihan, "Estimation of the effective self-diffusion tensor from the NMR spin echo," *Journal of Magnetic Resonance*, vol. B, no. 103, pp. 247–254, 1994.

[2] P.J. Basser, J. Mattiello, and D. LeBihan, "MR diffusion tensor spectroscopy and imaging," *Biophysical Journal*, vol. 66, no. 1, pp. 259–267, 1994.

[3] D. Tuch, "Q-ball imaging," *Magnetic Resonance in Medicine*, vol. 52, no. 6, pp. 1358–1372, 2004.

[4] M. Descoteaux, E. Angelino, S. Fitzgibbons, and R. Deriche, "Regularized, fast, and robust analytical q-ball imaging," *Magnetic Resonance in Medicine*, vol. 58, pp. 497–510, 2007.

[5] I. Aganj, C. Lenglet, G. Sapiro, E. Yacoub, K. Ugurbil, and N. Harel, "Reconstruction of the orientation distribution function in single- and multiple-shell q-ball imaging within constant solid angle," *Magnetic Resonance in Medicine*, vol. 64, no. 2, pp. 554–566, 2010.

[6] Antonio Tristan-Vega, C.-F. Westin, and Santiago Aja-Fernandez, "A new methodology for the estimation of fiber populations in the white matter of the brain with the funk-radon transform," *NeuroImage*, vol. 49, pp. 1301–1315, 2010.

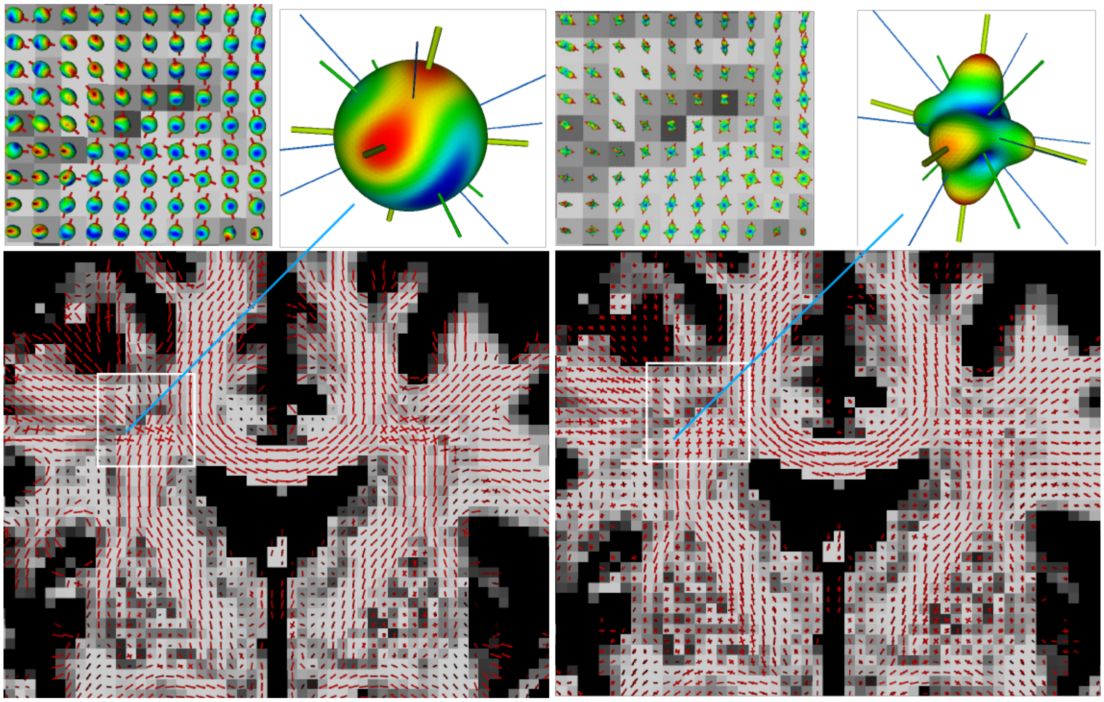

Fig. 2. Real Data Crossings: Maxima from ODF-T (left) & ODF-SA (right) in SH basis. Top: Maxima and ODFs. Bottom: Maxima extracted from ODF-Ts (left), and ODF-SAs (right). Zoom on a particular voxel with 3 fiber directions with the detected and classified extrema. Notice the greater number of crossings and sharper peaks in ODF-SA. Although the peaks in the ODF-T are subtle (indicated by the glyph colour), the maxima extraction method is still able to detect these peaks. Glyph-colour: red indicates high anisotropy (local peak), blue indicates low anisotropy (local trough). (Voxel) Line-colour: thick-green: Maxima, thin-green: Minima, fine-blue: Saddle points

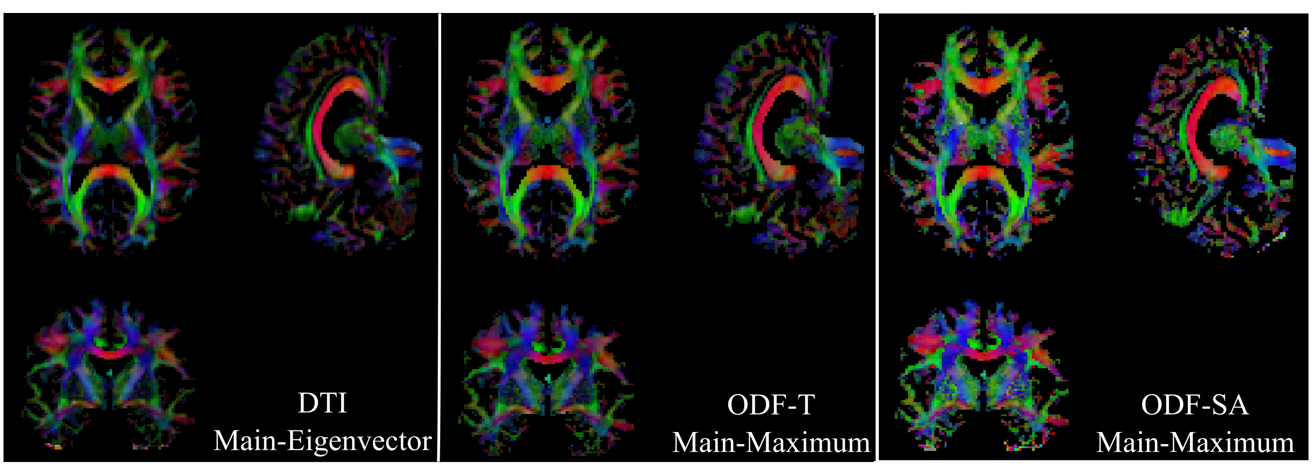

Fig. 3. RGB representation: red:X, green:Y, blue:Z. Left: DTI eigenvector, brightness: FA. Centre: ODF-T maximum, brightness: corresponding PFA-T. Right: ODF-SA maximum, brightness: corresponding PFA-SA. Notice the similarity.

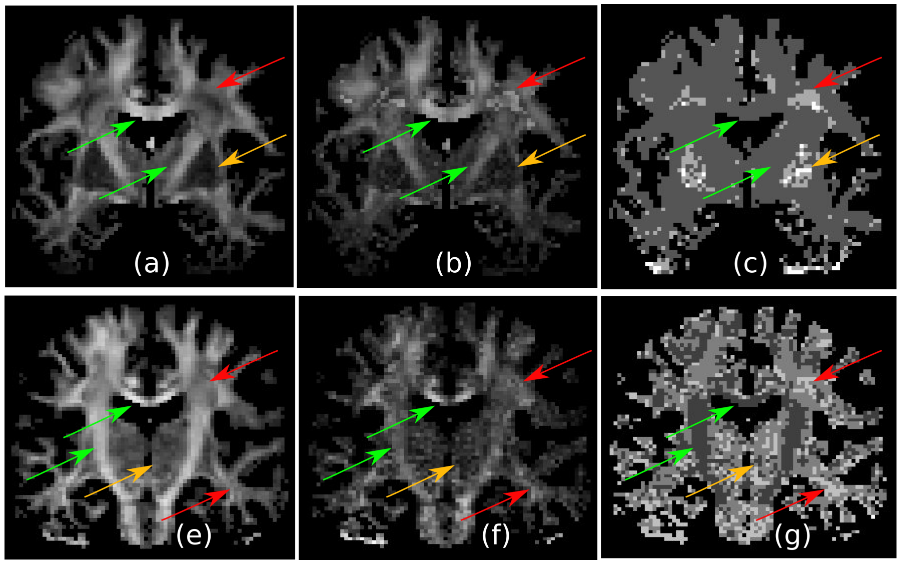

Fig. 4. Total-PFA and GFA. Top-row: ODF-T, Bottom-row: ODF-SA. 1st column: GFA from (a) ODF-T and (e) ODF-SA. 2nd column: Total-PFA – (b) Total-PFA-T from ODF-T (f) Total-PFA-SA from ODF-SA. 3rd column: Number-of-maxima from (c) ODF-T and (g) ODF-SA. Total-PFA measures the starriness or peakedness of an SF and emphasizes local sub-voxel anisotropy. Green arrow indicates regions with no crossings (dark in 3rd col.) but high local anisotropy (bright in Total-PFA) like the CC and the CST. Red arrow indicates regions with many crossings (bright in 3rd col.) and with high local anisotropy (bright in Total-PFA) like where the CC, CST and SLF intersect. However, these regions have low GFA values. Orange arrow indicates regions with high crossings (bright in 3rd col.) but with low local anisotropy (dark in Total-PFA). These regions also have low GFA values.

[7] K. M. Jansons and D. C. Alexander, "Persistent angular structure: new insights fom diffusion magnetic resonance imaging data," *Inverse Problems*, vol. 19, pp. 1031–1046, 2003.

[8] J.-D. Tournier, F. Calamante, D.G. Gadian, and A. Connelly, "Direct estimation of the fiber orientation density function from diffusion-weighted mri data using spherical deconvolution," *NeuroImage*, vol. 23, pp. 1176–1185, 2004.

[9] Luke Bloy and Ragini Verma, "On computing the underlying fiber directions from the diffusion orientation distribution function," in *MICCAI '08: Proceedings of the 11th international conference on Medical Image Computing and Computer-Assisted Intervention - Part I*, Berlin, Heidelberg, 2008, pp. 1–8, Springer-Verlag.

[10] Aurobrata Ghosh, Elias Tsigaridas, Maxime Descoteaux, Pierre Comon, Bernard Mourrain, and Rachid Deriche, "A polynomial based approach to extract the maxima of an antipodally symmetric spherical function and its application to extract fiber directions from the orientation distribution function in diffusion mri," in *Proceedings of Workshop on Computational Diffusion MRI, MICCAI 2008*, 2008.

[11] Iman Aganj, Christophe Lenglet, and Guillermo Sapiro, "Odf maxima extraction in spherical harmonic representation via analytical search space reduction," in *MICCAI (2)*, Tianzi Jiang, Nassir Navab, Josien P. W. Pluim, and Max A. Viergever, Eds. 2010, vol. 6362 of *Lecture Notes in Computer Science*, pp. 84–91, Springer.

[12] M. Descoteaux, E. Angelino, S. Fitzgibbons, and R. Deriche, "Apparent diffusion coefficients from high angular resolution diffusion imaging: Estimation and applications," *Magnetic Resonance in Medicine*, vol. 56, pp. 395–410, 2006.

[13] Bernard Mourrain and Jean-Pascal Pavone, "Subdivision methods for solving polynomial equations," *Journal of Symbolic Computation*, vol. 44, pp. 292–306, 2009.

[14] E.K. Im, "Hessian sufficiency for bordered hessian," *Res. Lett. Inf. Math. Sci.*, vol. 8, pp. 189–196, 2005.

[15] M. Descoteaux, E. Angelino, S. Fitzgibbons, and R. Deriche, "A linear and regularized odf estimation algorithm to recover multiple fibers in q-ball imaging," Tech. Rep. 5768, INRIA Sophia Antipolis, Nov. 2005.

[16] A. Anwander, M. Tittgemeyer, D. Y. von Cramon, A. D. Friederici, and T. R. Knosche, "Connectivity-based parcellation of broca's area," *Cerebral Cortex*, vol. 17, no. 4, pp. 816–825, 2007.